[PS]Complex Carbonate Pore Systems of the Carboniferous Hodder Mudstone Formation, Bowland Basin, UK*

Timothy M. Ohiara[1], Kevin G. Taylor[2], and Patrick J. Dowey[2]

Search and Discovery Article #51399 (2017)**
Posted August 7, 2017

*Adapted from poster presentation given at AAPG 2017 Annual Convention and Exhibition, Houston, Texas, April 2-5, 2017

[1]School of Earth and Environmental Science, The University of Manchester, Manchester, United Kingdom (timothy.ohiara@postgrad.manchester.ac.uk)
[2]School of Earth and Environmental Science, The University of Manchester, Manchester, United Kingdom

Abstract

Pores in shales or mudstones are mostly submillimetre-scale pores hosted in and around inorganic constituents and in mature organic matter residues. Micrometre– and nanometer– scale pores between and within particles of carbonate-rich sequences are strongly influenced by carbonate mineral diagenesis. The Lower Carboniferous Hodder Mudstone Formation in the Bowland Basin is a potential UK shale-gas play and provides an opportunity to understand the compositional controls on porosity in an organic- and carbonate-rich mudstone. This is achieved through the characterisation of pore types and mineral components from a suite of wells along the northern margin of the Bowland Basin. The work utilises petrographic, XRD, X-ray CT, and N_2 gas-adsorption techniques.

Samples were divided into nine lithofacies which provided a framework to establish compositions, textures, pore types, and depositional environments. Lithofacies were then grouped into associations: (A1) clay-rich mudstones – >50 % clay-sized particles; (A2) – calcareous silt-rich mudstones, and (A3) Skeletal calcareous mudstones. A1 (~40% of samples) exhibited rare planar to convolute laminae, but were mostly unlaminated. A2 (~30 % of samples) were largely unlaminated, but where A2 lithofacies grade into A1 they formed discontinuous ripple laminations. A3 (~30 % of samples) exhibited ripple laminations except for the rare occurrences of storm-brecciated, crinoidal beds within mudstones. Within the cores, lithofacies fine upwards from coarse-grained bioclast-rich mudstones to medium grained silt-rich mudstones and then fine-grained organic-rich mudstones.

Pore types included interparticle, intercrystalline, and intraparticle forms. Macropores (>4mm) exhibited vuggy intercrystalline pore morphologies within veins localised in the calcisiltites; while micro- to nano-pores (<62.5μm) occurred within pyrite framboids (intraparticle), between clay minerals and grains (interparticle) and in organic matter particles. In the clay-rich mudstones, pores within pyrite framboids and clay minerals were <300nm in diameter and comprised a large percentage of the pore volume. The skeletal calcareous mudstones exhibited <1μm sized-pores due to carbonate cementation and pore-filling kaolinite. Despite modifications made by early and late diagenesis, pore analysis show that porosity in the Hodder Mudstone is primarily controlled by compositional variation of detrital and biogenic grain

assemblages. The importance of this work is in characterisation of the pore structures within a potential future UK shale-gas play and in the identification of process controls in carbonate-dominated mudstones.

References Cited

Andrews, I.J., 2013, The Carboniferous Bowland Shale Gas Study: Geology and Resource Estimation: British Geological Survey for Department of Energy and Climate Change, London, UK, 56 p.

Clarke, H., P. Turner, and R.M. Bustin, 2014, Unlocking the Resource Potential of the Bowland Basin, NW England: Society of Petroleum Engineers - European Unconventional Resources Conference and Exhibition 2014, Unlocking European Potential, 2 February 2014, p. 25-27.

Dean, M.T., M.A.E. Browne, C.N. Waters, and J.H. Powell, 2011. A Lithostratigraphical Framework for the Carboniferous Successions of Northern Great Britain (onshore): British Geological Survey Research Report RR/10/07, 174 p.

Desbois, G., J.L. Urai, and P.A. Kukla, 2009, Morphology of the Pore Space in Claystones – Evidence from BIB/FIB Ion Beam Sectioning and Cryo-SEM Observations: eEarth Discussions, v. 4/1, p. 1-19.

Evans, D.J., and G.A. Kirby, 1999, The Architecture of Concealed Dinantian Carbonate Sequences over the Central Lancashire and Holme Highs, Northern England: Proceedings of the Yorkshire Geological Society, v. 52/3, p. 297-312.

Fraser, A.J., and R.L. Gawthorpe, 1990, Tectono-Stratigraphic Development and Hydrocarbon Habitat of the Carboniferous in Northern England: Geological Society, London, Special Publications, v. 55/1, p. 49-86.

Fraser, A.J., A.J. Nash, R.P. Steele, and C.C. Ebdon, 1990, A Regional Assessment of the Intra-Carboniferous Play of Northern England: *in*: J.J. Brooks (ed.), Classic Petroleum Provinces: Geological Society Special Publication 50, p. 417-440.

Jarvie, D.M., 2012, Shale Resource Systems for Oil and Gas: Part 1 - Shale-Gas Resource Systems, *in* J.A. Breyer (ed.), Shale Reservoirs - Giant Resources for the 21st Century, American Association of Petroleum Geologist Memoir 97, p. 69-87.

Loucks, R.G., R.M. Reed, S.C. Ruppel, and U. Hammeset, 2012, Spectrum of Pore Types and Networks in Mudrocks and a Descriptive Classification for Matrix-Related Mudrock Pores: American Association of Petroleum Geologists Bulletin, v. 96/6, p. 1071-1098.

Ma, L., K.G. Taylor, P.D. Lee, K.J. Dobson, P.J. Dowey, and L. Courtois, 2016. Novel 3D Centimetre-to Nano-Scale Quantification of an Organic-Rich Mudstone: The Carboniferous Bowland Shale, Northern England: Marine and Petroleum Geology, v. 72, p. 193-205. doi.org/10.1016/j.marpetgeo.2016.02.008

Macquaker, J.H.S., and A.E. Adams, 2003, Maximizing Information from Fine-Grained Sedimentary Rocks: An Inclusive Nomenclature for Mudstones: Journal of Sedimentary Research, v. 73, p.735-744.

Milliken, K.L., and M.E. Curtis, 2016, Imaging Pores in Sedimentary Rocks: Foundation of Porosity Prediction: Marine and Petroleum Geology, v. 73, p. 590.608. doi.org/10.1016/j.marpetgeo.2016.03.020

Milliken, K.L., M. Rudnicki, D.N. Awwiller, and T. Zhang, 2013, Organic Matter-Hosted Pore System, Marcellus Formation (Devonian), Pennsylvania: American Association of Petroleum Geologists Bulletin, v. 97/2, p. 177-200.

Modica, C.J., and S.G. Lapierre, 2012, Estimation of Kerogen Porosity in Source Rocks as a Function of Thermal Transformation: Example from the Mowry Shale in the Powder River Basin of Wyoming: American Association of Petroleum Geologists Bulletin, v. 96/1, p. 87-108.

Pommer, M., and K. Milliken, 2015, Pore Types and Pore-Size Distributions across Thermal Maturity, Eagle Ford Formation, Southern Texas: American Association of Petroleum Geologists, Bulletin, v. 99/9, p. 1713-1744.

Waters, C N, R.A. Waters, W.J. Barclay, and J.R. Davies, 2009, Lithostratigraphical Framework for Carboniferous Successions of Southern Great Britain (Onshore): British Geological Survey Research Report, RR/09/01, 184 p.

COMPLEX CARBONATE PORE SYSTEMS OF THE CARBONIFEROUS HODDER MUDSTONE FORMATION, BOWLAND BASIN, UK

Timothy Ohiara, Kevin Taylor, Patrick Dowey
University of Manchester, School of Earth and Environmental Sciences, University of Manchester, Manchester, M13 9PL, UK.
Timothy.ohiara@postgrad.manchester.ac.uk

The University of Manchester

100 AAPG ANNIVERSARY ACE 2017 ANNUAL CONVENTION & EXHIBITION
2-5 April 2017 • Houston, TX • George R. Brown Convention Center

School of Earth and Environmental Sciences

Basin studies

1. INTRODUCTION

Pores in shales or mudstones are mostly submillimetre-scale pores hosted in and around inorganic constituents (Desbois et al 2009; Loucks at al 2012; Milliken et al 2013; Ma et al 2016) and in mature organic matter residues (Jarvie 2012; Modica and Lapierre 2011; Loucks 2012; Ma et al 2016). Micrometre– and nanometer– scale pores between and within particles of carbonate-rich sequences are mostly lost during carbonate mineral diagenesis.

A question remains on the process controls of pore development in carbonate-dominated, organic– rich Carboniferous Hodder Mudstone which is a potential shale-gas resource in the Bowland Basin. A range of analytical techniques have been combined to capture the wide range of pore sizes hosted in the Carboniferous Hodder mudstones and its relation to mineral distribution.

This work is consequently aimed at characterising **macro- to nano- complex pore systems** within a potential carbonate-rich UK shale-gas play with relation to carbonate mineral diagenesis.

The objectives include:

- **A petrographic characterization of sedimentary lithofacies within core samples from 11 wells along a 3.7 km transect of the Hodder Mudstone**
- **Producing a high resolution qualitative descriptions and quantitative data on pore morphologies and size distributions**
- **Evaluating the effects of carbonate mineral diagenesis on pore evolution and preservation**
- **Establishing the economic implications of carbonate mineral diagenesis in a potential Carboniferous Bowland shale gas reservoir**

2. STUDY AREA

The Bowland Basin is a NE – SW – oriented half graben located in Lancashire, north-western UK. The map (figure 1) shows the Basin location with significant UK shale gas exploration wells (**Preese hall 1, Thistleton 1, Elswick 1**) and the location of sampled **Marl Hill Moor (MHD)** wells (red box Figure 1) north-east of the exploration wells. Wells are shown in Figure 4, section 3.

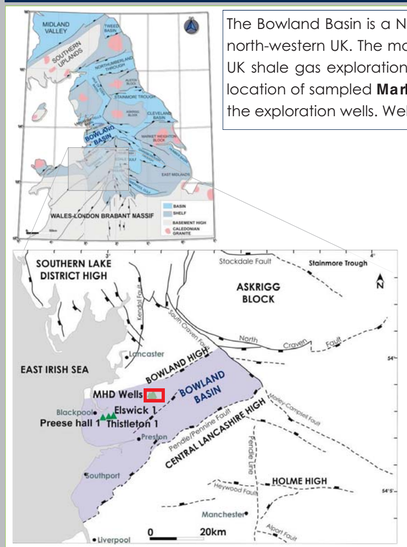

Figure 1: Bowland basin location map adapted from Evans and Kirby (1999); map inset shows Carboniferous (Visean) syn-rift structural element (modified after Fraser et al 1990).

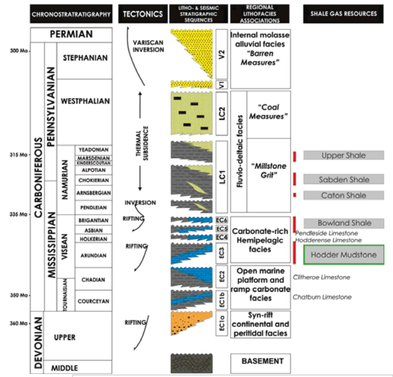

Figure 2: Summarized stratigraphy of the East Midlands and the Pennine potential shale gas resource. Modified after Fraser and Gawthorpe (1990) and Dean et al. (2011)

- Bowland basin holds an estimated **1300 TCF** of total original gas in place (Clarke et al. 2014)
- The gas-bearing section is **>6000ft (1800m)** thick unit of Visean to Namurian strata, predominantly hemipelagic mudstones and thinly laminated calcareous turbidites deposited in a mid to outer ramp setting (Fraser and Gawthorpe 1990; Andrew 2013)
- The Hodder mudstone forms the lower section of the Carboniferous Bowland-Hodder Shale Gas play in the Basin
- TOC varies from 2-4 wt. % and Tmax 450 (top) – 610 (base) (Andrews 2013)
- Complex structural evolution during to active rifting in late Devonian-Visean times resulted in natural open and mineralised fractures in the Basin (Fraser and Gawthorpe 1990)

3. RESEARCH DATA AND METHODS

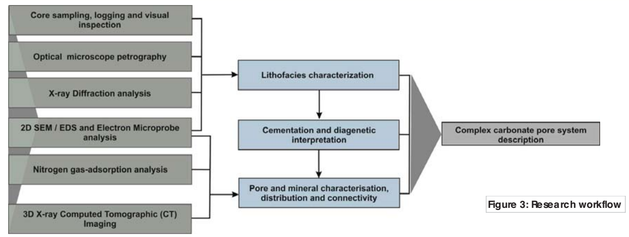

Figure 3: Research workflow

Figure 4: Research dataset

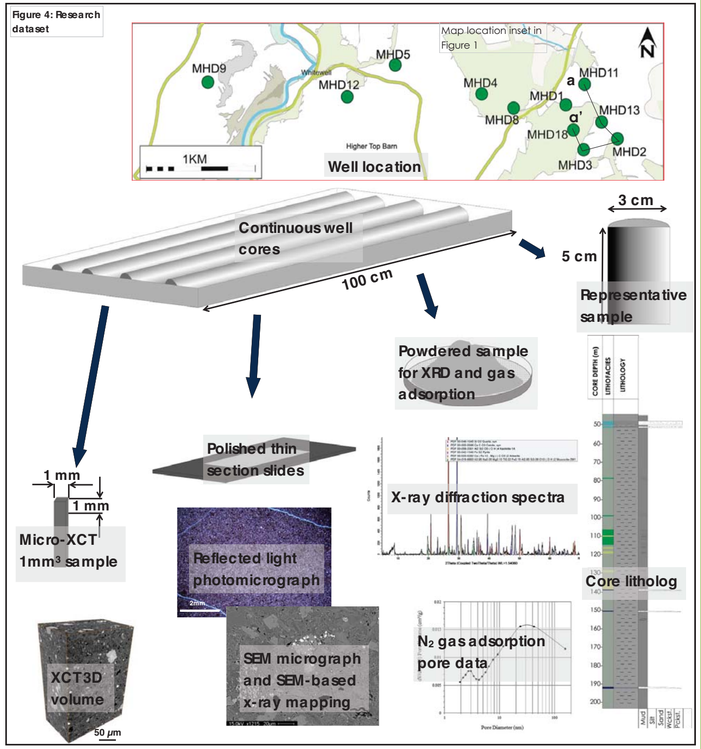

- A total of 1,679 metres (5,508 Ft) of continuous well cores from 11 wells have been logged for this study. These cores were acquired onshore during a solid mineral exploration project from the uplifted section of the basin (**figure 4**)
- 131 samples were selected across the Hodder lithostratigraphic sequence using core logs to guide sample selection (**figure 4**) for thin section, XRD, N_2 gas adsorption and X-ray CT
- 50 oriented, polished, thin sections with blue epoxy impregnation were prepared from samples
- Thin sections were studied using light and scanning electron microscopy (SEM)
- Pore data was collected using N2 Gas adsorption techniques from 10 representative powdered samples using Micrometritics 3Flex surface characterisation analyser
- 3D X-ray tomographic images were acquired using XT H 225, Nikon X-ray tomography system. Data was processed using the Avizo 3-D visualization software (FEI).

4. LITHOFACIES

The textural terminologies utilized in this study were adapted from the Macquaker and Adams (2003) classification of mudstones on the basis of percentage composition of constituent grains irrespective of provenance. Suffixes "-dominated", "–rich" and "-bearing" are used as descriptive modifiers to indicate percentage composition >90%, 50-90% and 10-50% respectively of clay, silt or skeletal materials present. The classification is further modified by the addition of prefixes denoting sedimentary structures and/or textures present. Nine core lithofacies types (**LF1 – LF9**) have been recognised and grouped into three lithofacies association (**A1, A3, A3**) based on relative compositional variation.

A1	A2	A3
Clay-rich mudstone (> 50% clay-sized particles)	**Silt-rich mudstones (>50% silt-sized particles)**	**Skeletal calcareous mudstones (>50% Bioclast fragments)**
Convolute-laminated silt-bearing clay-rich mudstone **(LF2)**	Unlaminated silt-rich mudstone **(LF6)**	Poorly-laminated bioclast rich mudstone **(LF8)**
Planar-laminated silt-bearing clay-rich mudstone **(LF3)**	Ripple-laminated silt-rich mudstone **(LF7)**	Ripple-laminated bioclast rich mudstone **(LF9)**
Unlaminated clay-rich mudstone **(LF4)**		Unlaminated Bioclast-dominated mudstone **(LF5)**
		Mottled bioclast-dominated mudstone **(LF1)**

Figure 5: Simplified illustration of the Hodder Mudstone lithofacies stacking pattern. Grading from bioclastic-rich mudstones to clay-rich sequences (A3- A2- A1).

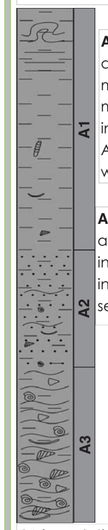

A1: Fine-grained, largely hemipelagic deposits in a relatively low energy muddy open-marine setting. These mudstones are intermittently interrupted by sediment slump beds. A1 constitutes the distal lithofacies within the basin

A2 forms an intermediate lithofacies association with a characteristic intercalation of fine– silty grained interturbidites and hemipelagic clay sediments

A3 is a relatively proximal lithofacies association from resedimented mechanically abraded limestones deposited by turbidity current

Figure 6 shows core photos taken from MHD 3 showing a relatively complete succession of the lithofacies association

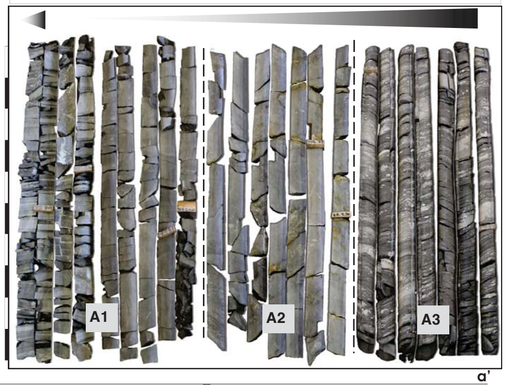

Figure 7

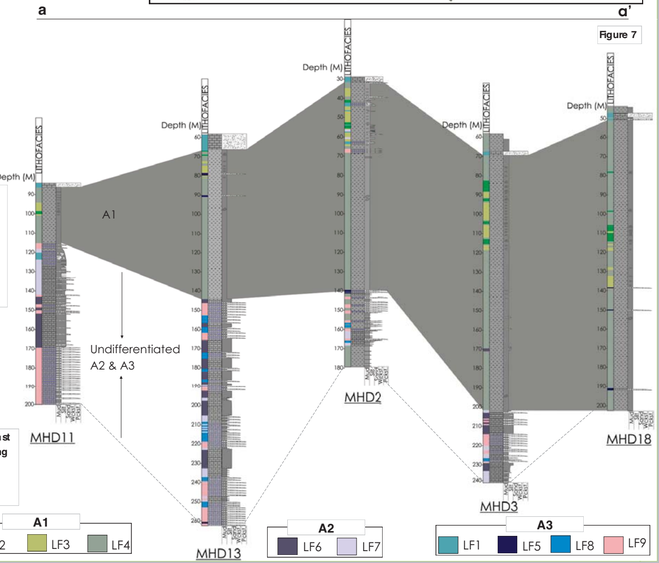

Figure 7 is a well transect a-a' to the south-east of the study area (Figure 4) showing increasing thickness of A1 (LF2, LF3, LF4) and irregular depositional pattern of A2 (LF6, LF7) and A3 (mostly LF5, LF 8 and LF9)

COMPLEX CARBONATE PORE SYSTEMS OF THE CARBONIFEROUS HODDER MUDSTONE FROMATION, BOWLAND BASIN, UK

MANCHESTER 1824

AAPG

School of Earth and Environmental Sciences

Basin studies

5. TEXTURE, MINERALOGY AND POROSITY

i) A1– CLAY-RICH MUDSTONES

Core photos | Photomicrographs in cross-polarised light | ESEM BSE micrographs

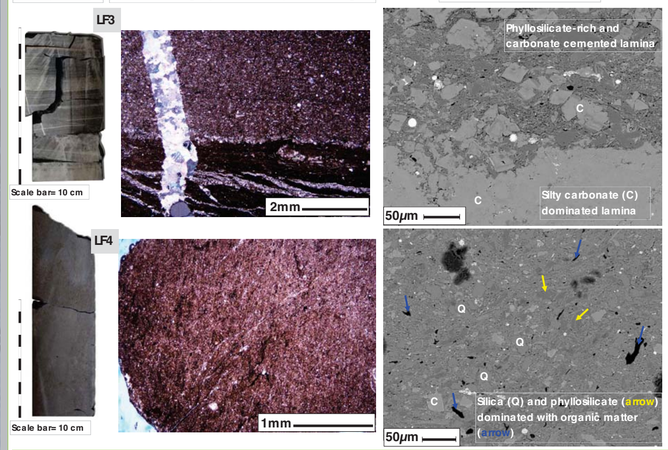

ii) A2– SILT-RICH MUDSTONES

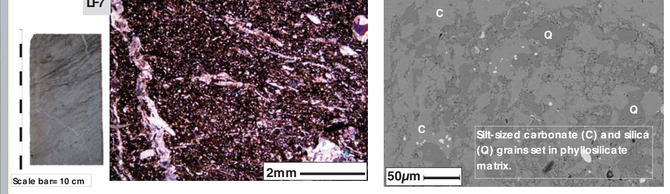

iii) A3– SKELETAL CALCAREOUS MUDSTONES

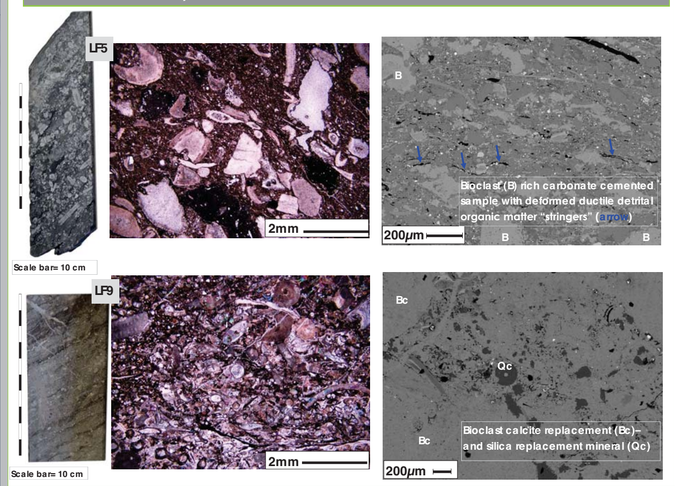

XRD BULK MINERALOGY

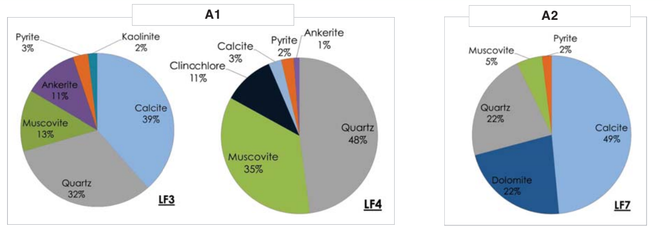

- The Hodder Mudstone on average from XRD and image data is a calcareous mudstone (3%-81% carbonate content) with varying clay and silt-sized **quartz**, **pyrite**, and phyllosilicate content (**muscovite**, **kaolinite**, **chlorite** and **albite**)
- **Lithofacies Association A1** exhibits massive– (LF4) to planar– (LF3) and convolute– (LF2) laminated clay-rich mudstones with carbonate components mostly of calcite in clay-sized particles, bioclast fractions and crystalline sparry calcite cement
- Sections with high concentration of carbonate content within A1 (example LF 3) reflects the presence of calcite, dolomite, ankerite and rarely siderite. These components are due to the network of carbonate and ferroan carbonate fractures within the lithofacies.
- **Lithofacies Association A2** has predominantly silt-sized grains of quartz, calcite and dolomite with clay-sized matrix of muscovite, kaolinite and albite. This association is intensely fractured with veins of calcite, dolomite, ferroan calcite, ferroan dolomite and barite.
- **Lithofacies association A3** has >50% fraction of coarse-grained skeletal fragments mostly of calcite composition. These grains are set in ripple clay-rich laminae. This unit justifies the significant increase in carbonate content towards the base of the formation. Grouped under A3 are also 5cm to 130cm units of debris flow deposits with high skeletal fragment composition that are found mostly interbedded and overlying A1 (LF1 and LF 5 respectively)

MICRO X-RAY CT VOLUME MINERAL SEGMENTATION

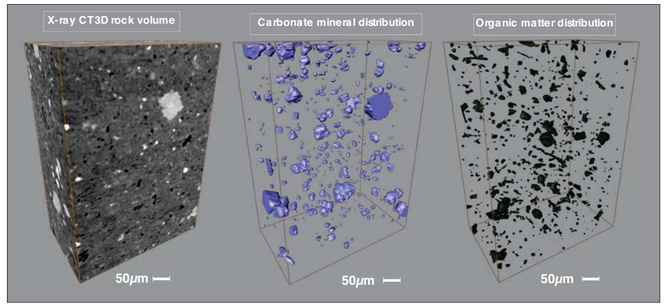

- 3D image analysis from representative A1 sample (LF4) shows carbonate mineral distribution caused by the presence of skeletal debris in fine-grained muddy matrix. Fragments are mostly from crinoids, bivalves, brachiopods, gastropods benthonic foraminifers and calcareous algae
- Total organic carbon (TOC) content which has an average measured value of 1.4wt% occurs as primary (detrital) organic matter and secondary or migrated residual hydrocarbon and bitumen.

MICROPORE (<63μm) MORPHOLOGY FROM DIGITAL IMAGE ANALYSIS

Intercrystalline pores	Intraparticle pores	Interparticle pores
These are pores between phyllosilicate cleavage planes, termed intraplatelet pores by Louck et al 2012	These are pores between framboidal pyrite crystals	These occur as dissolution pores in psuedomorphic calcite cements within partially cemented bioclast grains	These pores take different forms around and in-between grains as intergranular pores (Loucks et al 2012) or circumgranular pores (Milliken and Curtis 2016)

Interparticle and intercrystalline pores

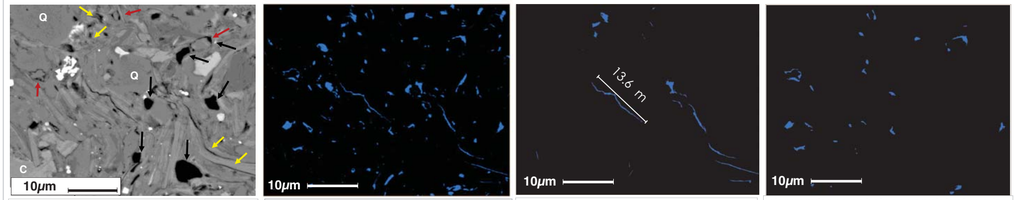

BSE micrograph of a calcareous clay-rich mudstone. Sample from LF4

Average pore surface area = 3.14%

Phyllosilicate-hosted pores in muscovite and clay minerals (arrows in BSE Image)

Intergranular pores between crystals of quartz and ductile clay minerals (arrows in BSE image)

Intraparticle pore

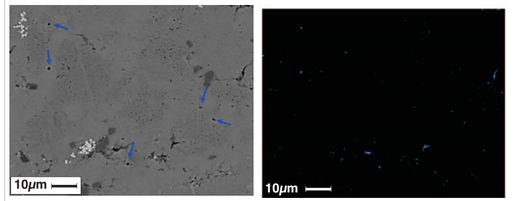

Dissolution intragranular pores

Average pore surface area = 0.99%

- The average micropore surface area of interparticle and intercrystalline pores after statistical pixel filtering of 2D SEM images is about 3%
- These intercrystalline (yellow arrows) and interparticle pores (red arrows) comprise a large percentage of the pore area
- Most intergranular pores have relatively large pores size and occur as wedge-shapes pores between rigid grains and ductile clay particles
- Elongate intercrystalline pores can propagate for about 13 m with a pore diameter of <300nm
- These pores are in most cases occupied by either detrital or secondary organic matter (black arrows)
- Dissolution micropores (blue arrows), are sparsely distributed in replacement texture-type cements. Average pore size in dissolution pores is ~1 m
- Organic matter hosted pores were not visible during this analysis

NANOMETRE-PORE SIZE (2nm—300nm) DISTRIBUTION USING N_2 GAS ADSORPTION

Lithofacies Association	Representative lithofacies	Pore Specific Surface Area-BET SA (m^2/g)	Pore Volume (1.7-300nm diameter) (cm^3/g)	Average Pore Width (nm)	Possible pore Type
A1	LF3	10.3	0.025	12.18	Intergranular and intercrystalline
	LF4	21.1	0.030	8.40	Intergranular and intercrystalline
A2	LF7	3.2	0.012	15.72	Intergranular and intercrystalline
A3	LF5	8.7	0.019	9.90	Intergranular
	LF9	2.6	0.010	15.478	Dissolution-Intragranular

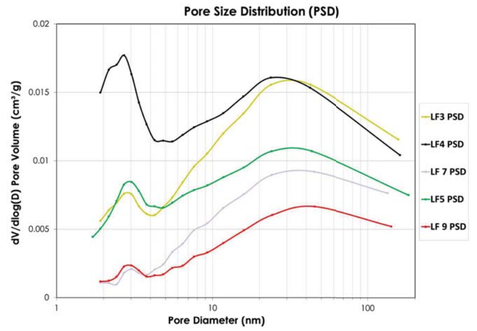

- A substantial amount of pore volume does exist in nanopore scale and is mostly dominated by mesopores (2-50nm sized pores; IUPAC nomenclature)
- There is a constant bimodal distribution of pore diameters in all measurer samples reflecting an abundance of 2-3nm sized pores and 20-50nm sized pores
- The average volume of nanopores (1.7-300nm diameter) per gram of sample is about 0.030 cm^3 hosted by LF4– A1
- Fine-grained, well-sorted and macro fossil-lean rock units retain the best appreciable nanopore (1.7-300nm diameter) volume
- Although pore sizes within the finer grained well sorted mudstones are relatively small, they are abundant and make up substantial volume of micropores within the studied succession
- LF5 being bioclastic rich has a relatively higher pore volume and diameter compared to other carbonate-rich lithofacies LF9 and LF7. This is due to its presence within clay-dominated lithofacies (LF4), attributed to episodic slump sediment deposition

COMPLEX CARBONATE PORE SYSTEMS OF THE CARBONIFEROUS HODDER MUDSTONE FROMATION, BOWLAND BASIN, UK

MANCHESTER 1824

AAPG

School of Earth and Environmental Science

Basin studies

6. PORE VARIATION WITHIN LITHOFACIES

A1

- Clay-rich sequences (A1) are dominated by particles <5 m, these constituents include rigid sparry calcite (C), quartz (Q) crystals and phyllosilicate clay minerals
- Grain sorting and bending of ductile phyllosilicates around the rigid granular grains preserves wedge-shaped micropores as shown in figures A and B (black arrows)
- Phyllosilicate bending also results in grain-splitting along cleavage planes. Micropores of this nature have been observed in the Hodder mudstone (Figure A, white arrow) and also by Pommer & Milliken (2015) in the Eagle Ford Shale
- Appreciable fraction of nanometre-sized pores exist between kaolinite "booklets" and chlorite platelets which are prominent within this facies association
- These matrix related pores with the addition of intercrystaline pores in pyrite framboids make up a large percentage of the pore volume in A1

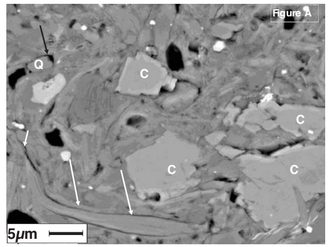

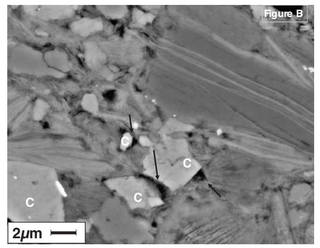

A2

- Pores within A2 are proportional to the ratio of silty carbonate and quartz fractions to clayey components (Figure C)
- Relatively well sorted silt-dominated sections exhibit poor micropore volume due to fabric arrangement favourable to contact dissolution and cementation (Figure D)
- However, in some case where there is a high level of dolomite precipitation, interparticle dissolution-rim pores (loucks et al 2012) occur around the edges of rigid rhombohedral dolomite crystals when in direct contact with clay particles (Figure E).

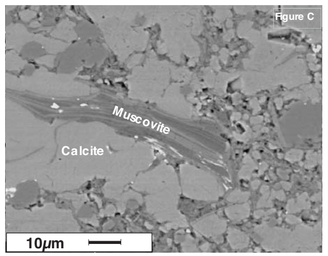

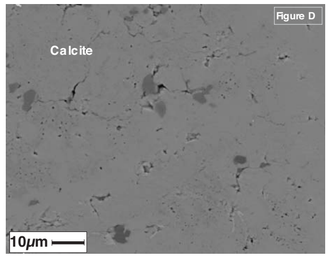

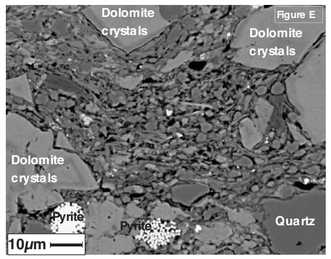

A3

- Due to increased ratio of calcareous particles to clay materials, carbonate cements are pervasive in A3 and are largely pseudomorphic in texture, assuming textures of early diagenetic kaolinite
- Pore-filling calcite and dolomite cements are observed replacing kaolinite "booklets" (kao. Figure F) and filling intercrystalline pores between "booklets"
- Primary pores often results when soft tissues of calcareous organisms dissolve (Loucks et al 2012; Pommer and Milliken 2015; Milliken and Curtis 2016). However, these pose are rarely preserved in carbonate-rich units due to calcite and dolomite mineral precipitation (Figures F and G)
- Pseudomorph of calcite and dolomite (dol. Figure F) in cavities left by decayed soft tissues of fossils are common in bioclast –rich units (A2 and A3)

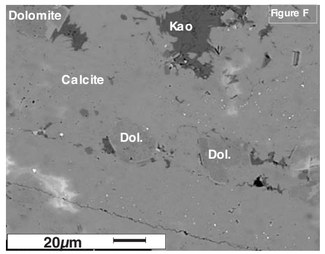

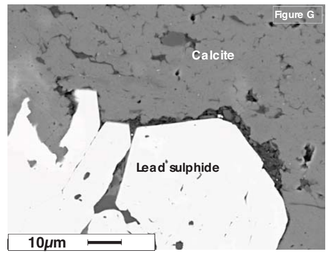

6. FRACTURE PORES

- Pore associated with fractures also contribute to the total pore volume. The propagation of these fractures have been observed to be lithofacies controlled.
- There is varied intensity of both open and closed fractures in the Hodder Mudstone. Mineralized veins due to differing generations alternate in diameter from single centimetre-thick vertical, horizontal and inclined veins to a complex network of millimetre – to micrometre—thick veins
- Veins are mostly of calcite, dolomite, ferroan calcite, ferroan dolomite and barite minerals dominate association A2
- These carbonate—rich sequences exhibit vuggy intercrystalline pores of up to 4mm in diameter within localised veins (Figures A and B, this section)
- Millimetre to micrometre thick veins are most prominent in clay-rich sequences (A1) and are mostly calcite fractures with weak contacts around fracture walls. These fractures do not host pores but provide lines of weakness when they propagate along bedding planes of laminated lithofacies (LF3)
- Occasionally, fracture are stained with hydrocarbon, indicative of active petroleum conduit systems (Figure 6 of section 4)

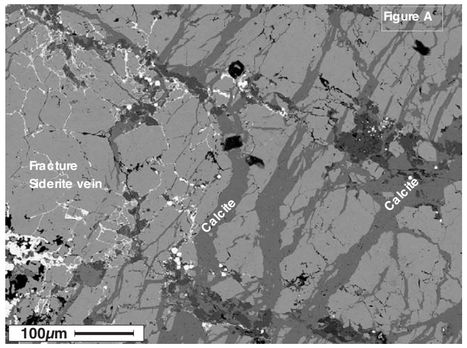

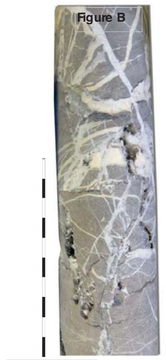

7. CONCLUSION

- Nine lithofacies make up the Hodder Mudstone Formation. These lithofacies are grouped into three associations (A1, A2 and A3) based on compositional variability
- Association A1 is mostly clay-rich with limited amount of carbonate content (<10% on average)
- A2 is dominated by silt-sized particles of mostly quartz, calcite and dolomite set in clay matrix
- A3 is highly calcareous with skeletal debris in significant turbiditic texture
- Pores exist in interparticle, intercrystalline and intraparticle forms (Loucks et al 2012)
- Macroscopic and two-dimensional SEM observations with Nitrogen gas adsorption analysis show that pores in Hodder Mudstone range from 3nm to >5cm
- Despite modifications made by early and late diagenesis, this research shows that porosity in the Hodder Mudstone is primarily controlled by compositional variation of detrital and biogenic grain assemblages
- Lithofacies association A1 has the largest amount of pore volume hosted within and around mineral fractions
- The effect of carbonate mineral diagenesis on pore development is controlled by initial primary constituent, hence, calcite/dolomite cement precipitation and resultant reduction in pore volume is pronounced in highly calcareous lithofacies A2 and A3. The figures A and B below show a typical comparison between two samples from A1 and A3 in response to pore preservation.

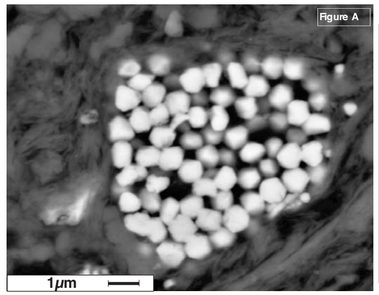

Pyrite framboids are easily seen and abundant in the Hodder mudstone. They can hold substantial pore volume. But, their preservation depends on the associated minerals.

Figure A and B show contrasting response to a similar kind of pore (pyrite-hosted intercrystalline pore) preservation due to pronounced variability in carbonate content.

Pores of this nature are better preserved in clay-rich sequences than in carbonate rich sequences.

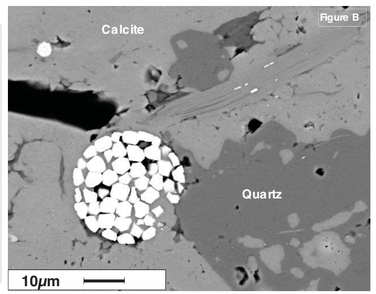

Summary Illustration:

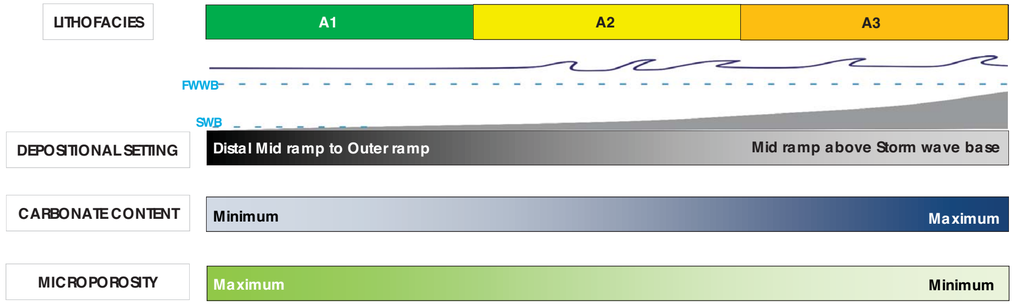

8. FUTURE WORK

- The effects of mechanical abrasion on thin sections may influence porosity identification. Focused Ion Beam polished sections will be prepared and studied.
- Further analyses will focus on the characterization of OM-hosted pores
- XRF, SEM-cathodoluminescence imaging and electron microprobe analysis will be undertaken to further characterise the timing of paragenetic events.
- Additional gas adsorption data to characterize the variability in and between lithofacies.

9. REFERENCES

- Andrews, I.J., 2013. British Geological Survey for Department of Energy and Climate Change, London, UK.
- Clarke, H., Turner, P. & Bustin, R.M., 2014. *SPE - European Unconventional Resources Conference and Exhibition 2014: Unlocking European Potential, 2(February), pp.25–27*
- Dean, M.T.; Browne, M. A. E.; Waters, C. N. & Powell, J. H., 2011. *British Geological Survey Research Report RR/09/01, p.174*
- Desbois, G., Urai, J.L. & Kukla, P.A., 2009. *eEarth Discussions, 4(1), pp.1–1.*
- Evans, D.J. & Kirby, G.A., 1999. *Proceedings of the Yorkshire Geological Society, 52(3), pp.297–312*
- Fraser, A.J. & Gawthorpe, R.L., 1990. *Geological Society, London, Special Publications, 55(1), pp.49–86*
- Fraser, A.J.; Nash, A. J.; Steele, R. P. & Ebdon, C. C., 1990. *A regional assessment of the intra-Carboniferous play of northern England J. J. Brooks, ed. Classic Petroleum Provinces, 50, pp.417–440*
- Jarvie, D.M., 2012. *Shale reservoirs—Giant resources for the 21st century, 97, pp.69–87*
- Loucks, R.G. et al., 2012. *AAPG Bulletin, 96(6), pp.1071–1098*
- Ma, L. et al., 2016. *Marine and Petroleum Geology, 72, pp.193–205*
- Macquaker, J.H.S. & Adams, A.E., 2003. *Journal of Sedimentary Research, 73, pp.735–744*
- Milliken, K.L. & Curtis, M.E., 2016.*Marine and Petroleum Geology, 73, pp.590–608*
- Milliken, K.L. et al., 2013. *AAPG Bulletin, 97(2), pp.177–200*
- Modica, C.J. & Lapierre, S.G., 2012. *AAPG Bulletin, 96(1), pp.87–108*
- Pommer, M. & Milliken, K., 2015. *AAPG Bulletin, 99(9).*